JAST, Vol. 12, No. 1, pp. 65-74

JAST
Journal of Aerospace Science and Technology

A Numerical Study on the Aeroacoustic Radiation from a Finite Length Rotating Cylinder

H.R. Talesh Bahrami[1], S. Ghasemlooy[2] and H. Parhizkar[3*]

1. School of Mechanical Engineering, Iran University of Science and Technology

2, 3. MalekAshtar University

Postal Code: Tehran, IRAN

hparhiz@mut.ac.ir

Rotating cylinders have wide applications in different areas, especially the aerodynamic area. However, the acoustic behaviors of these components have not been widely studied. The generating noise from a spinning cylinder is mainly due to the detached vortices from the leeward of the body. In this study, the large eddy simulation technique is used to simulate the flow field over a three-dimensional cylinder. In the following, the Ffowcs Williams and Hawkings equation is used to estimate the noise at the specified locations using the oscillating pressure components on the cylinder wall. The acoustic behavior of both stationary and rotating cylinders are studied. Results show that the acoustic behaviors of cylinders rotating with smaller frequencies (up to f=16f0, where f0 is the dominant detaching frequency of vortices on a stationary cylinder) are nearly the same. However, at higher rotational frequencies (24f0) where vortices are omitted, OASPL of the generated noise is reduced considerably (about 20 dB at different angles with constant radial positions, r=26D, at mid-span plane). On the other hand, when the rotational frequency is increased over this limit, the pressure oscillation on the wall becomes significant and the OASPL approaches higher values.

Keywords: Rotating Cylinder, Aerodynamic Noise, Large Eddy Simulation, Ffowcs Williams and Hawkings, Acoustic

Introduction

The potential aerodynamic and hydrodynamic advantages of a spinning cylinder or a Magnus rotor have attracted the engineers and scientists attentions to explore its practical applications in the recent decades. Seifert [1] reviewed the recent attempts in using Magnus rotors in industrial proposes. As well as, numerous studies have been conducted to investigate the flow field past a rotating cylinder. The main purposes of these studies are the understanding of the wake dynamics[2], using rotational movement as a controlling technique[3], utilizing the produced Magnus force[4], or enhancing heat transfer [5]. For example, Tokumaru and Dimotakis [6] experimentally showed that the structure of wakes behind a cylinder could be controlled effectively by subjecting it to a rotating cylinder placed at thetandem position. Kussaiynov and et al. [4] studied the aerodynamic performance of a rotating cylinder as components of a windmill operating based on the Magnus effect. Their results show that the drag and lift forces of the spinning cylinder depend on the Reynolds number. They have demonstrated that an increase in the flow velocity results in a reduction in the lift and drag forces by 5-10%.

Although investigations on the aerodynamic characteristics of rotating cylinders are very extensive in the literature, studies on the acoustic behavior of this fundamental problem are very rare.

1. PhD
2. Assistant professor
3. Associate Professor (Corresponding Author)

The most investigations on the acoustic radiated from spinning cylinders are focused onthose are positioned in a quiescent medium or inviscid flow. This problem has an analytical solution in some conditions[7, 8]. For example, Farhadi [9] recently presented a semi-analytical solution for calculatingthe radiated acoustic from rotating and non-rotating finite-length cylinders. He assumed that the cylinder is immersed in an irrotational inviscid compressible flow. Although analytical solutions give a good insight into the problem, they have limited applications. In the real conditions and at high Reynolds fluid flows where three-dimensional vortices detach from the cylinder irregularly, the flow field becomes so complicated. In these conditions, only some especial solutions of three dimensional Navier-Stokes equations could be simulated the flow fieldwith an acceptable accuracy. For example, the large eddy simulation (LES) of the flow field in conjunction with Ffowcs Williams and Hawkings (FW-H) equation have been used extensively to predict the acoustic radiated from a stationary cylinder immersed in a high Reynolds flow. Zhang et al. [10] experimentally and numerically studied effects of changing the cylinder surface to a wavy structure on the reduction of the propagatedaeroacoustic noise. They used the LES technique to simulate the flow field and FW-H equation to predict the emitted noise. Their results show that the aerodynamic noise of the wavy cylinder is reduced by 6.7 dB as compared with a smooth cylinder. Liu et al. [11] used the same strategy to predict the propagated aerodynamic sound radiated from a porous coated cylinder. Their results show that porous media could effectively reduce the aerodynamic noise.

The review of the literature shows that rotating cylinders have very potential applications in different areas. As well as, different studies have been conducted to predict the aerodynamic noise radiated from a stationary cylinder using Navier Stokes equations, LES technique, and FW-H equation. However, according to the authors' knowledge, no theoretical study has been conducted to investigate the aerodynamic noise radiated from a spinning cylinder. In this investigation, a numerical study has been done to study the aerodynamic noise of a rotating cylinder using the LES technique along with FW-H equation. In the first step, a stationary cylinder is studied to achieve a reasonable insight into the problem. In this section, the source directivity of the generated sound is studied. In the next step, different non-dimensional rotational frequencies of the rotation are studied. Results are inspected using contours and diagrams.

Governing equations and boundary conditions

The schematic of the problem is given in Fig. 1. The diameter of the cylinder is d=0.019 m. It is placed in a uniform flow with a Mach number 0.2. The corresponding Reynolds number calculated based on the inflow velocity and the cylinder diameter is 90,000. The computational domain is a rectangular cube where the distance of the cylinder from the left-hand side boundary, where the flow enters the domain (inlet), is 4D. The distance of the cylinder from the downstream boundary (outlet) is 26D. The inlet and outlet boundary conditions are velocity inlet and pressure outlet, respectively. The side boundaries are symmetry conditions. The cylinder could oscillate rotationally according to the problem conditions. The grid used in this study is given in Fig. 2. Quadrilateral cells are used in the mid-span plane because of their less numerical diffusion with respect to unstructured triangular grids. The grid is cooper in the depth of the domain which is a repeat of the mid-span grid in the z-direction.

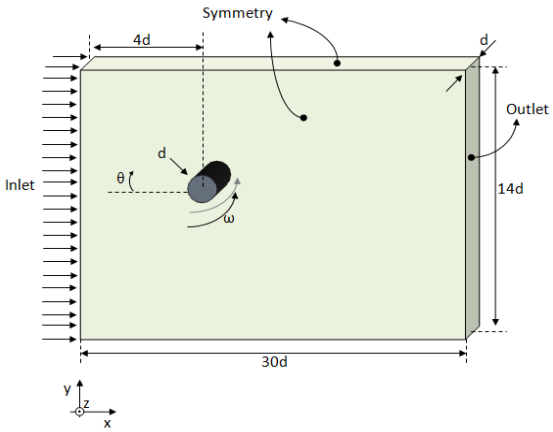

Fig. 1. The schematic of the problem

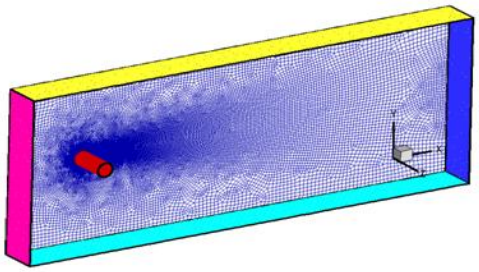

Fig. 2. The grid generated in the domain

The aerodynamic noise emitted from the cylinder surface into the uniform flow can be predicted in two steps. In the first one, the LES technique is used to simulate the flow field and subsequently, the generated noise in the observer location is estimated using the FW-H equation and the pressure fluctuations at the surface of the cylinder[12].

In the LES technique, the filtering operation is performed on the time-dependent variables. In this procedure, eddies with scales smaller than the filter width which is employed in the computations are filtered out. Consequently, the achieved equations estimate the dynamics of large eddies. In this technique, a filtered variable which is expressed by an over-bar is found as follows [13]:

$$\overline{\varphi}(x) = \int_{\Omega} \varphi(x')G(x,x')dx' \tag{1}$$

where φ is a transient variable which filtering operation is performed on it, $\overline{\varphi}$ is the filtered variable, Ω is the fluid domain where the filtering operation is performed there, G is the filter function which determines the scale of resolved eddies, x' is the spatial coordinate, and x is the filtered spatial coordinate. The filtering operation can be performed using a volume averaging of the variable in the cell volume as follows [14]:

$$\overline{\varphi}(x) = \frac{1}{V}\int_{V} \varphi(x')dx' \; \acute{x} \in v \tag{2}$$

Consequently, the domain Ω appeared in Eq. (1) is V in Eq. (2) and the filter function is [14]:

$$G(x,\acute{x}) = \begin{cases} \dfrac{1}{V'}, & x' \in v \\ 0, & x'otherwise \end{cases} \tag{3}$$

In the following, the filtering operations explained previously are used to find the essential equations of the LES technique.

By performing the filtering operation, the filtered continuity equation appears as follows [15]:

$$\frac{\partial \rho}{\partial t} + \frac{\partial \bar{u}_i}{\partial x_i} = 0, \tag{4}$$

The filtered momentum equations are obtained using Navier-Stokes equations as follows [15]:

$$\frac{\partial(\bar{u}_i)}{\partial t} + \frac{\partial \overline{u_i u_j}}{\partial x_j} = \frac{\partial}{\partial x_j}\left(\nu \frac{\partial \sigma_{ij}}{\partial x_j}\right) - \frac{1}{\rho}\frac{\partial \bar{p}}{\partial x_i} \quad i, j = 1,2,3 - \frac{\partial \tau_{ij}}{\partial x_j}, \tag{5}$$

where σ_{ij} is the stress tensor due to molecular viscosity, which isfound as follows:

$$\sigma_{ij} = \mu\left(\frac{\partial \bar{u}_i}{\partial x_i} + \frac{\partial \bar{u}_j}{\partial x_j}\right) - \frac{2}{3}\mu\frac{\partial \bar{u}_i}{\partial x_i}\delta_{ij} \tag{6}$$

where δ_{ij} is the Kronecker delta.

In incompressible flows, the momentum equations can be simplified as follows:

$$\frac{\partial(\bar{u}_i)}{\partial t} + \frac{\partial \overline{u_i u_j}}{\partial x_j} = \frac{\partial}{\partial x_j}\left(\nu\left(\frac{\partial \bar{u}_i}{\partial x_i} + \frac{\partial \bar{u}_j}{\partial x_j}\right)\right) - \frac{1}{\rho}\frac{\partial \bar{p}}{\partial x_i} - \frac{\partial \tau_{ij}}{\partial x_j} \tag{7}$$

where the subgrid-scale stress tensor,τ_{ij}, is often estimated as follows [16]:

$$\tau_{ij} - \frac{1}{3}\tau_{kk}\delta_{ij} = -2\mu_t \bar{S}_{ij} \tag{8}$$

where $\bar{S}_{ij}$and $\mu_t$are the rate-of-strain tensor for the resolved scale and the subgrid-scale turbulent eddy viscosity, respectively. Performing a simple dimensional analysis, Eq. 8 can be expressed as follows [14]:

$$\mu_t = L_s^2\left|\bar{S}_{ij}\right| = L_s^2\sqrt{2\bar{S}_{ij}\bar{S}_{ij}} \tag{9}$$

where

$$L_S = \min(\kappa d, C_s\bar{\Delta}) \tag{10}$$

and

$$\bar{\Delta} = (\Delta x \Delta y \Delta z)^{1/3} \tag{11}$$

Furthermore, C_s is the Smagorinsky constant assumed 0.1 in this investigation, d is the distance to the closest cell wall, and κ is the von Karman constant.

As previously mentioned, the FW-H equation is used in this investigation to estimate the aerodynamic noise. This method only can be only used to approximatethe noise emitted by a surface into an open environment. In fact, it cannot predict the sound reflections due to a secondary surface

other than the sound source [17]. The FW-H equation can be obtained by manipulating Navier-Stokes equations. More information about deriving the FW-H equation can be found in Refs. [18, 19]. The FW-H equation is a non-homogeneous wave equation expressed as follows:

$$\begin{aligned}&\frac{1}{c_\infty^2}\frac{\partial^2 \mathrm{p}'}{\partial \mathrm{t}^2}-\nabla^2 \mathrm{p}'\\&=\frac{\partial}{\partial \mathrm{t}}\{[\rho_\infty \mathrm{v_n}+\rho(\mathrm{u_n}-\mathrm{v_n})\delta(\mathrm{f})]\}\\&-\frac{\partial}{\partial \mathrm{x_i}}\{[\rho_{\mathrm{ij}}\mathrm{n_j}\\&+\rho \mathrm{u_j}(\mathrm{u_n}-\mathrm{v_n})\delta(\mathrm{f})]\}\\&+\frac{\partial^2}{\partial \mathrm{x_i}\,\partial \mathrm{x_i}}\{\mathrm{T_{ij}H(f)}\}\end{aligned} \tag{11}$$

where u_i is the velocity component in the direction x_i, $\mathrm{p}'=\mathrm{p}-\mathrm{p}_\infty$, $\mathrm{v_n}$ and u_n are velocity components perpendicular to the surface (f=0), H(f) is the Heaviside function, and δ(f) is the Dirac delta function. In this procedure, a mathematical surface is defined as S surrounding the exterior boundary of the problem. Subsequently, the parameter f is defined where f<0 and f>0 respectively showsthe inside and outside of the surface.c_∞ is the sound velocity of the free stream, n_i is the normal vector on the exterior boundary of the surface, and $\mathrm{T_{ij}}$ is the Lighthill stress tensor which is written as follows:

$$\begin{aligned}T_{ij}=\ &\rho u_i u_j+P_{ij}\\&-C_\infty^2(\rho\\&-\rho_\infty)\delta_{ij}\end{aligned} \tag{12}$$

where

$$\begin{aligned}P_{ij}=P\delta_{ij}-\mu\Bigg[&\frac{\partial \bar{u}_i}{\partial x_j}+\frac{\partial \bar{u}_j}{\partial x_i}\\&-\frac{2}{3}\frac{\partial u_k}{\partial x_j}\delta_{ij}\Bigg]\end{aligned} \tag{13}$$

A pressure based scheme is utilized in the simulation. The implicit fractional time step is exploited as the pressure segregated algorithm. The second-order upwind techniques are used to discretize convection terms. The unsteady CFD is performed with a non-dimensional time-step of $\frac{\Delta t U_{inf}}{d}=0.00367$. It is selected carefully so that the Courant–Friedrichs–Lewy (CFL) number becomes less than unity nearly over the entire computational domain.

Validation

The experimental results of Ref. [17] are used to check the validity of the current acoustic simulation procedure. This investigation is performed on a stationary cylinder with diameter 0.019 m and length 25.3 times of the diameter. The velocity of the free stream is 69.2 m/sec and the Reynolds number is 90000 calculated based on the cylinder diameter. The Reynolds of the flow is higher than the critical Re ($\mathrm{Re}\geq 1\times 10^5$) where the flow detaches behind the cylinder and a vortex shedding occurs at Strouhal number about 0.2 [17]. A receiver is placed at 128d far from the cylinder at ❑=90 with respect to windward stagnation line.

The grid resolution is achief parameter in the LES technique. The grid must be as fine as possible in the neighborhood of the cylinder wall in all directions including the flow direction, perpendicular to the wall and in the depth of the domain (direction z in Fig. 1). Consequently, the CFD simulation of very long objects with enough accuracy needsa considerable computational cost. The previous investigations have revealed that the pressure distribution in the depth of a cylinder varies periodically. Therefore, to decrease the computational cost, a smaller cylinder could be simulated and the resultingpropagated sound is related to a longer cylinder by performinga proper sound pressure level correction. Investigations have shown that the correction value depends on the frequency as follows [20]:

$$\begin{aligned}&\Delta SPL_{\mathrm{corr}}(\omega)\\&=\begin{cases}10\log\left(\frac{L}{L_s}\right) & L_c(\omega)\leq L_s\\ 10\log\left(\frac{L_c(\omega)}{L_s}\right)+20\log\left(\frac{L}{L_c(\omega)}\right) & L_s\leq\ L_c(\omega)<L\\ 20\log\left(\frac{L}{L_s}\right) & L\leq L_c(\omega)\end{cases}\end{aligned} \tag{14}$$

where L is the experimental or actual length of object, $\mathrm{L_s}$ is the length of the simulated object and $\mathrm{L_c}$ is the coherence length found using coherence function:

$$\Gamma_{ij}(\omega)=\frac{\overline{Re(\hat{P}_i\hat{P}_j)}}{\sqrt{\left|\hat{P}_i\right|^2}\sqrt{\left|\hat{P}_j\right|^2}} \tag{15}$$

where $\hat{P}_i$ and $\hat{P}_j$ are pressure perturbations in the frequency domain at different span locations on the object. If pressure components on two different locations fluctuate with the same phases, the equivalent coherence function is unity. The coherence function is zero if fluctuations are independent otherwise it lies in the range $0<\Gamma_{ij}(\omega)<1$. According to Kato et al. [20], where the coherence function becomes

0.5 is called the coherence length. The coherence length maybe even longer than the actual length while it is desirable to simulate a length much smaller than the actual length according tothe computational cost considerations. In these conditions, Kato et al. [20] proposed to compute the coherence length using an extrapolation with a Gaussian function,exp $(-\Delta z^2/L_c^2)$, where Δz is the distance between two different locations on the span of the object. In the current validation process, the length of the cylinder is considered 2.5d. The variation of Γ_{ij} of St=0.19 is depicted in Fig. 3. It can be noted that the coherence length is greater than the experimental length of the cylinder. Consequently, the third relation is given in Eq. 15 must be used to adjust the numerical results. According to Eq. 15, the sound pressure level correction is found about 22 dB for the current case.

The comparison of the sound pressure level of the current investigation and that of Revellet al. [17] is shown in Fig. 4. It can be noted that the simulation and the experiment are in good agreement although they become different in St<0.18. This discrepancy may probably due to the error noise in the experimental results. Nevertheless, it can be seen that the simulation could estimatewell the Strouhal number of largely detached vortices at St=0.19. In addition, the OASPL reported by Revell et al. [17] is 100 dB while the OASPL predicted in the current investigation by applying the correction is 103 dB. In summary, it can be concluded that the current simulation procedure could approximate well the experiment.

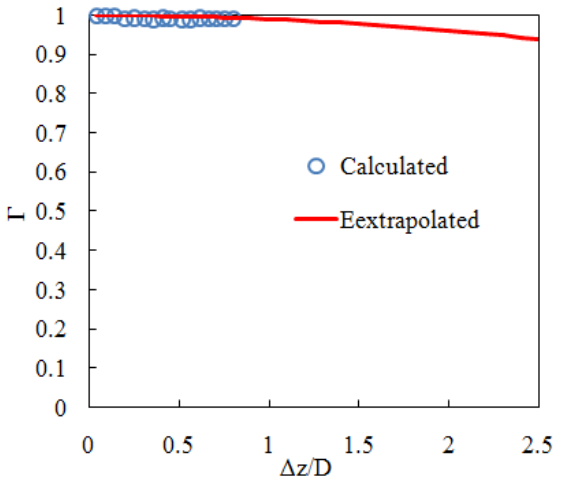

Fig. 3. Calculated and extrapolated coherence functionsversus the spanwise length

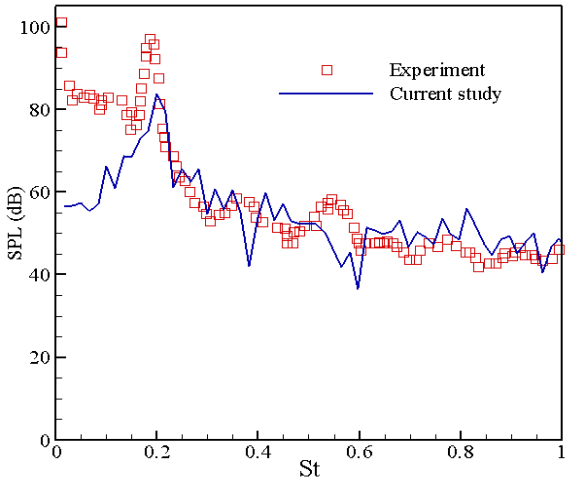

Fig. 4. The comparison of the sound pressure level of the current investigation and experimental results of Ref. [17]

Results and discussion

Stationary cylinder characteristics

When a vortex detaches from one side of the cylinder, a negative pressure region appearsin that side while a positive pressure region emerges inthe other side; successive vortex shedding from the upper and lower sides of the cylinder generates negative and positive pressure pulses alternately. This phenomenon produces sound pressure waves at the observation location [21] and oscillating drag and lift coefficients.The alternatevortices shedding from the upper and lower sides also affect the upstream pressure and velocity distribution on the cylinder surface because flow regime is in the subsonic region, the upper stream becomes aware of the events happening in the downstream.For example, the variation of upper and lower sides' pressure distributions and the related contours of the cylinder in different non-dimensional solution times (t*=tU/D) are given in Fig. 5. It can be seen that in some instants the upper side's pressure on

the cylinder wall is greater than the lower side and in some instants, this situation is reversed.

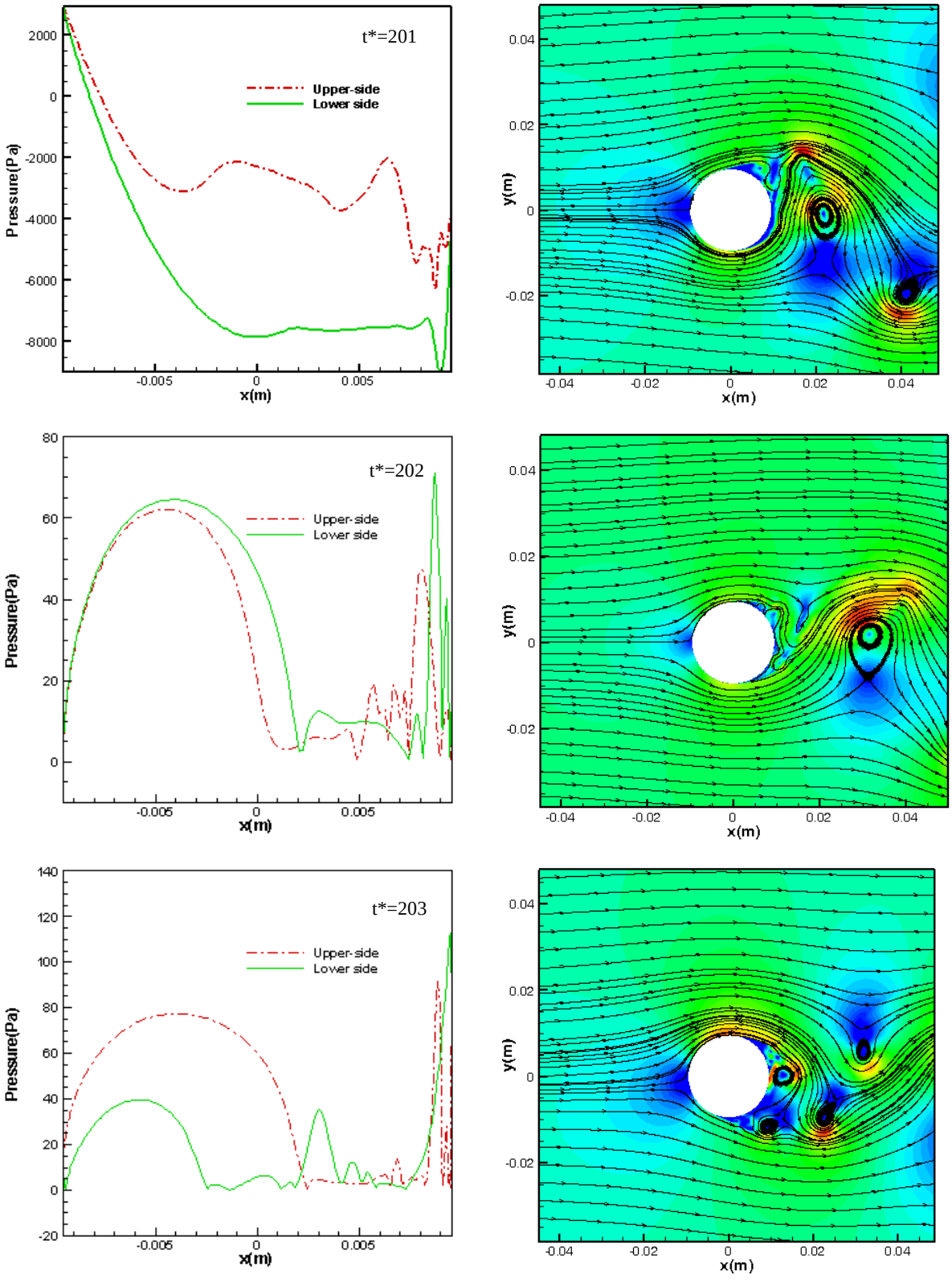

Fig. 5. Variation of the upper and lower sides pressure distribution and the related velocity contours (mid-span position)

The variation of the lift and drag coefficients and acoustic pressure with respect to the non-dimensional time are given inFig. 6. Drag and force coefficients are calculated using the shear stress and pressure forceexerted on the cylinder surface. It is worth mentioning that the vortex shedding is not started until about t*=100. After thistime, the solution goes through transient conditions and reaches quasi-steady conditions at longer solution times where vortex shedding becomes nearly periodical.The power spectral density of the lift coefficient and acoustic pressure are given in Fig. 6-b. It can be seen that several peaks at about the same frequencies present in both PSDs. It indicates that the lift coefficient and acoustic pressure are at the same phase which also can be qualitatively detected from Fig. 6-a. When a vortex sheds from one side of the cylinder, a negative pressure region is appeared there, which produces a positive lift force in that direction. Therefore, in the most part of Fig. 6-a, the lift and acoustic pressure vary in the opposite directions. The irregular variation of drag and lift forces may be due to the irregular three-dimensional breakup of the vortices originating from the leeward of the cylinder [22].

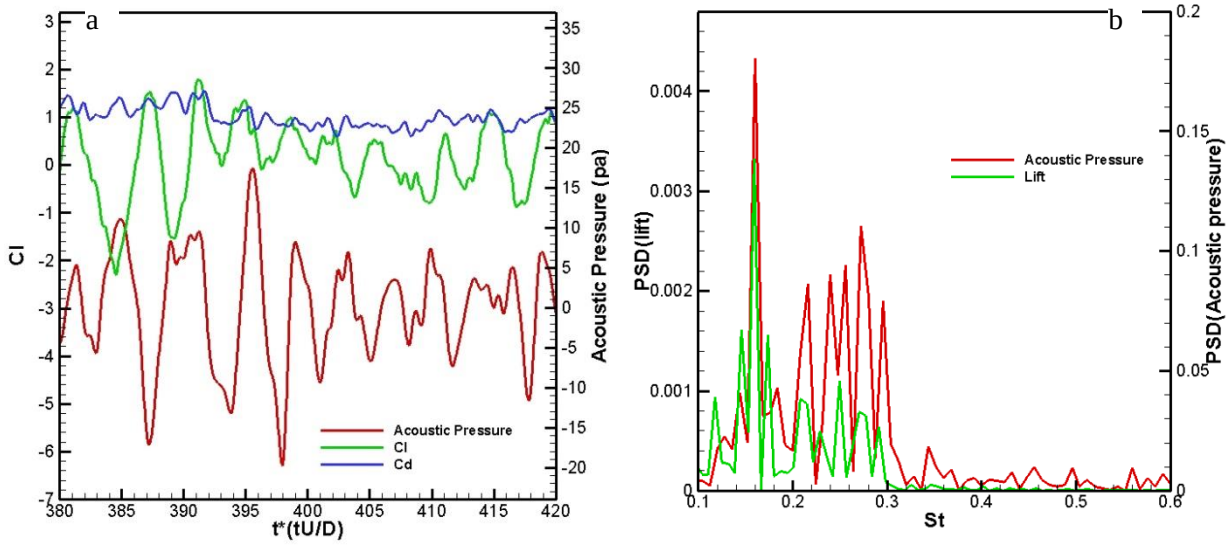

Fig. 6- a) The variations of lift coefficient and acoustic pressure with respect to time b) and spectral analysis of sound pressure at the observed point and lift coefficient

Fig. 7 shows a view of the OASPL directivity calculated at 36 observers, located on a circle in the mid-span of the x-y plane at r= 26D. In this problem, the main origin of the aerodynamic noise is dipole sources which are produced due to the force or momentum changes acting on the fluid [23]. The force or momentum exchange between the surface and the fluid is occurred due to the vortex shedding in the current problem. It can be seen that the OASPL of the stationary cylinder varies in a kidney shape in the ❑-direction which also confirms that the source is dipole. Dipole sources radiate sound non-uniformly in different directions. They have symmetry propagation structure, minimum strength in two directions, and maximum strength in the opposite directions from the theoretical point of view[24]. According to Fig. 6-a, the amplitude of the oscillations ofthe lift force is much higher than drag force. Therefore, the acoustic field is mainly due to the lift force oscillations and has a latitudinal structure.

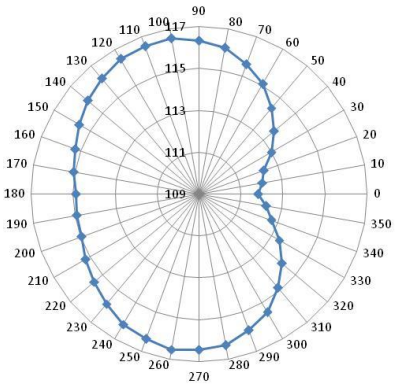

Fig. 7. The directivity of OASPL inradial distances26m in the mid-span plane

Rotating cylinder characteristics

A rotating cylinder has a non-zero velocity magnitude at its wall. This moving boundary changes the velocity profile near the cylinder which its behavior differs on the upper and lower haves of the cylinder. For example, in this problem where the cylinder rotates counterclockwise, the near flow field in the upper half of the cylinder is in the opposite direction of the main flow. On the other hand, in the lower half side, the near and main flow fields are in the same directions. However, in the low spinning rates of the cylinder, the near flow field resulting from the rotating wall is in a very narrow region and rapidly damped out or merged with the main flow. Furthermore, the near flow field is dominant in the high spinning rate. For example, the velocity contours and streamlines of two cases f=1f0 and f=28f0 is shown in Fig. 8-a and b.f0 is the dominant detaching frequency of vortices on the stationary cylinder.From Fig. 8-a, it can be seen that at low spinning rates of the cylinder, the near flow field is mainly due to the main flow. When the main flow approaches the back half of the cylinder, it encounters a sudden expansion andan adverse pressure gradient which forcesthe flow to be separated. Therefore, some vortices appear behind the cylinder. On the other hand, in the high spinning rates of the cylinder (Fig. 8-a, f=28f0), the near field flow becomes dominant and vortices disappear. In these conditions, a stagnation point appears on the top of the cylinder, which is the interaction of backward flow resulting from the near flow field and forward main flow. The stagnation point in the low spinning rates of the cylinder is located somewhere in the forehead of the cylinder.

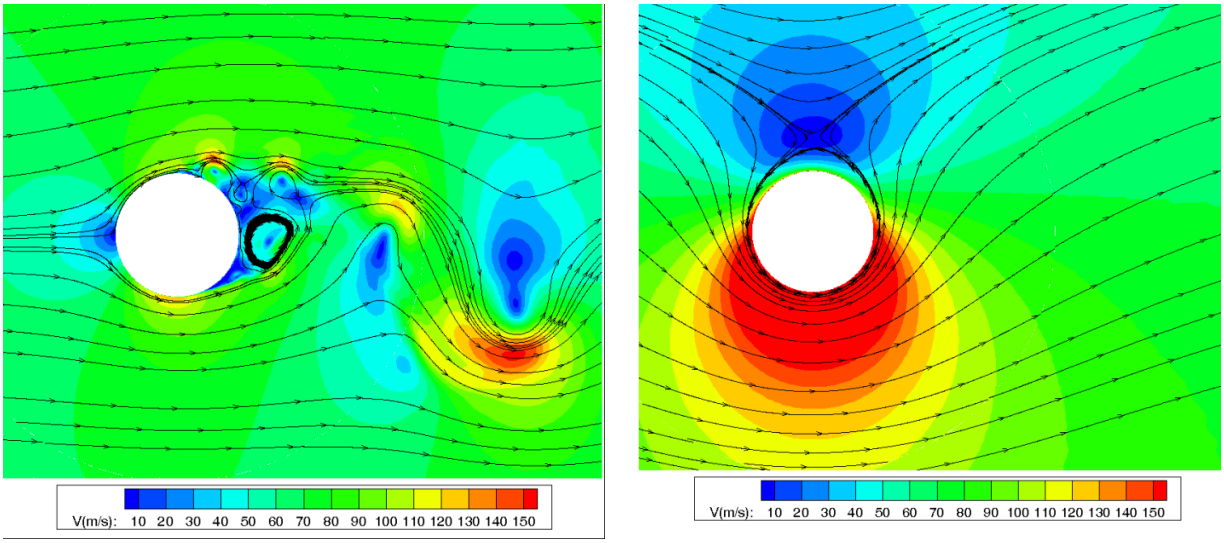

Fig. 8. Contours and streamlines of rotating cylinders with frequencies a) f=1f0, b)f=28f0

As mentioned earlier, the rotational movement of the cylinder wall could change the flow field around it. This outcome also alters the radiated acoustic behavior. The OASPL of the rotating cylinder at different rotational frequency and directions is given in Fig. 9. It can be seen that in low rotational frequencies (up to f=16f0) the main flow is dominant. Therefore, the major mechanism of producing acoustic noise is the samein all issues. Consequently, the overall spectral densities of acoustic radiation of different spinning cylinders are nearly the same.They differ only a few decibels in different rotational frequencies lower than16f0. However,

in higher rotational frequencies (for example 24f0), the near flow field becomes completely dominant and omits the vortices formation (as shown Fig. 8-b). Under these conditions, the main mechanism of aerodynamic noise production namely pressure oscillation due to downstream vortices on the cylinder wall does not exist. Therefore, as it can be considered from Fig. 9, the case f=24f0 has about 20dB lower overall spectral density than smaller rotational frequencies at different directions. However, by increasing rotational frequency greater than this limit (for example, f=28f0), due to higher momentum of the flow, the pressure oscillations on the cylinder wall becomes important and the OASPL increases. However, as it can be seen from Fig. 9, at soaring frequencies the directivity of the sound tends to diminishand the sound propagatesnearly equal in different directions.

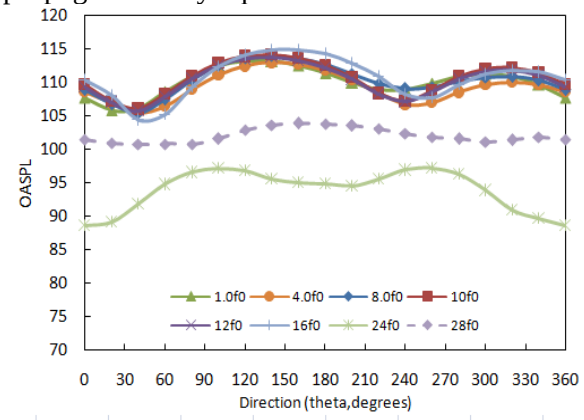

Fig. 9. The variation of OASPL with respect to the rotational frequency of the cylinder

Conclusions

Rotating cylinders have different potential applications. Aerodynamic and hydrodynamic behaviors of this apparatus have been investigated extensively in recent years. However, acoustic behavior of spinning cylinders is rare in the literature. In this study, the aerodynamic noise radiated from a three-dimensional cylinder is studied at Re=90000 and different rotational frequencies. The Large eddy simulation is used to simulate the flow field and capture the detached wakes with an acceptable accuracy. The pressure components presenting on the wall of the cylinder are used through Ffowcs Williams and Hawkings equation to estimate the aerodynamic noise at specified locations around the cylinder. The investigation is done both on the stationary and rotating cylinders. The study shows that the radiated noises in low rotational frequencies (lower than 16f0) are nearly the same directivity and values. However, in higher rotational frequencies (about 24f0) the radiated aerodynamic noise is reduced considerably with respect to a stationary cylinder or spinning cylinder with low rotational frequencies (about 20 dB at f=24f0). The main reason for this reduction may be due to the disappearing of vortices. However, when the rotational frequency is increased much higher than this limit, the aerodynamic noise increases.It may be due to the greater force and momentum exchange between the wall and flow because of the high momentum value of the main flow.

References

[1] J. Seifert, A review of the Magnus effect in aeronautics, Progress in Aerospace Sciences, 55 (2012) 17-45.

[2] S. Mittal, B. Kumar, Flow past a rotating cylinder, Journal of Fluid Mechanics, 476 (2003) 303-334.

[3] N. Shao, G. Yao, C. Zhang, M. Wang, A New Method to Optimize the Wake Flow of a Vehicle:The Leading Edge Rotating Cylinder, Mathematical Problems in Engineering, 2017 (2017).

[4] K. Kussaiynov, N. Kadyralievna Tanasheva, M. Miryusupovich Turgunov, G. Meiramovna Shaimerdenova, A. Ravshanbekovna Alibekova, The Effect of Porosity on the Aerodynamic Characteristics of a Rotating Cylinder, Modern Applied Science, 9(2) (2015).

[5] R.I. Elghnam, Experimental and numerical investigation of heat transfer from a heated horizontal cylinder rotating in still air around its axis, Ain Shams Engineering Journal, 5 (2014) 177–185.

[6] P. Tokumaru, P. Dimotakis, Rotary oscillation control of cylinder wake, Journal of Fluid Mechanics, 224 (1991) 77–90.

[7] W. Williams, N. Parke, D. Moran, C.H. Sherman, Acoustic Radiation from a Finite Cylinder, The Journal of the Acoustical Society of America, 36(12) (1964) 2316-2322.

[8] V.R. Lauvstad, Aerodynamic Sound Generated by a Rotating Cylinder, The Journal of the Acoustical Society of America, 43(6) (1968).

[9] S. Farhadi, Acoustic radiation of rotating and non-rotating finite length cylinders, Journal of Sound and Vibration, 428 (2018) 59-71.

[10] C.C. Zhang, W.Q. Wang, L. Shi, J. Wang, L.Q. Ren, Experimental and Numerical Study on Aerodynamic

Noise Reduction of Cylindrical Rod with Bionic Wavy Surface, in: Applied Mechanics and Materials, Trans Tech Publ, 2014, pp. 690-701.

[11] H. Liu, J. Wei, Z. Qu, Prediction of aerodynamic noise reduction by using open-cell metal foam, Journal of Sound and Vibration, 331 (2012) 1483–1497.

[12] D.L.H. J. E. Ffowcs-Williams, Sound generation by turbulence and surfaces in arbitrary motion, Philosophical Transactions of the Royal Society of London A: Mathematical, Physical and Engineering Sciences, 264(1151) (1969) 321-342.

[13] K. Mobini, M. Niazi, Large Eddy Simulation of the Flow across a Rotating Circular Cylinder International Journal of Fluid Mechanics Research, 41(1) (2014).

[14] L. Shi, C. Zhang, J. Wang, L. Ren, Numerical simulation of the effect of bionic serrated structures on the aerodynamic noise of a circular cylinder, Journal of Bionic Engineering, 9 (1) (2012) 91-98.

[15] H. Liu, J. Wei, Z. Qu, Prediction of aerodynamic noise reduction by using open-cell metal foam, Journal of Sound and Vibration, 331(7) (2012) 1483-1497.

[16] J. Smagorinsky, General circulation experiments with the primitive equations: I. The basic experiment, Monthly weather review, Monthly weather review, 91(3) (1963) 99-164.

[17] J.D. Revell, R.A. Prydz, A.P. Hays, Experimental study of airframe noise vs. drag relationship for circular cylinders, Aiaa Journal, 16(9) (1978) 152-165.

[18] J.S. Cox, K.S. Brentner, C.L. Rumsey, Computation of vortex shedding and radiated sound for a circular cylinder: subcritical to transcritical Reynolds numbers, Theoretical and Computational Fluid Dynamics, 12(4) (1998) 233-253.

[19] M. Zdravkovich, Flow around circular cylinders volume 1: fundamentals, Oxford University Press, Oxford

[20] C. Kato, A. Iida, Y. Takano, H. Fujita, M. Ikegawa, Numerical prediction of aerodynamic noise radiated from low Mach number turbulent wake, in: 31st Aerospace Sciences Meeting, 1993, pp. 145.

[21] O. Inoue, N. Hatakeyama, Sound generation by a two-dimensional circular cylinder in a uniform flow, Journal of Fluid Mechanics, 471 (2002) 285–314.

[22] D.A. Lysenko, I.S. Ertesvåg, K.E. Rian, Towards simulation of far-field aerodynamic sound from a circular cylinder using OpenFOAM, International Journal of Aeroacoustics, 13(1-2) (2014) 141-168.

[23] R.S. Matoza, D. Fee, T.B. Neilsen, K.L. Gee, D.E. Ogden, Aeroacoustics of volcanic jets: Acoustic power estimation and jet velocity dependence, Journal of Geophysical Research: Solid Earth, 118(12) (2013) 6269–6284.

[24] D.A. Russell, J.P. Titlow, Y.-J. Bemmen, Acoustic monopoles, dipoles,and quadrupoles: An experiment revisited, American Journal Of Physics Journal Of Physics, 67(8) (1999) 660-664.